Electronic supplementary information (ESI)

Nanostructured hexahedron of bismuth ferrite clusters: Delicate synthesis processes and efficient multiplex catalyst for the organic pollutant degradation

Zhong-Ting Hu[a]*, Shun Kuang Lua[b], Xiaoli Yan[a,c], Teik-Thye Lim[a]

[a] Division of Environmental and Water Resources Engineering, School of Civil and Environmental Engineering, Nanyang Technological University, 50 Nanyang Avenue, Singapore 639798, Singapore
[b] School of Material Science and Engineering, Nanyang Technological University, 50 Nanyang Avenue, Singapore 639798, Singapore
[c] Nanyang Environment and Water Research Institute (NEWRI), Nanyang Technological University, 1 Cleantech Loop, CleanTech One, Singapore 637141, Republic of Singapore.

* Corresponding author: E-mail: zhu009@e.ntu.edu.sg

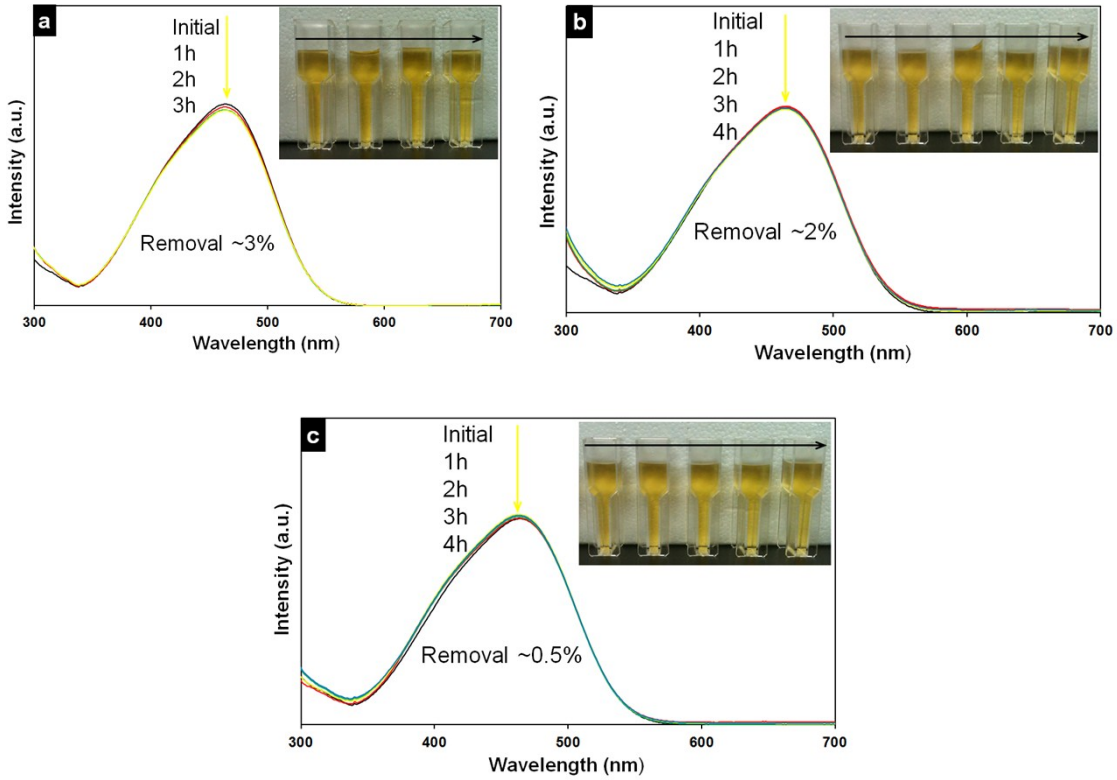

Fig. S1. Stability of MO under different conditions: (a) visible light with H_2O_2, (b) H_2O_2 in dark, (c) simulated solar.

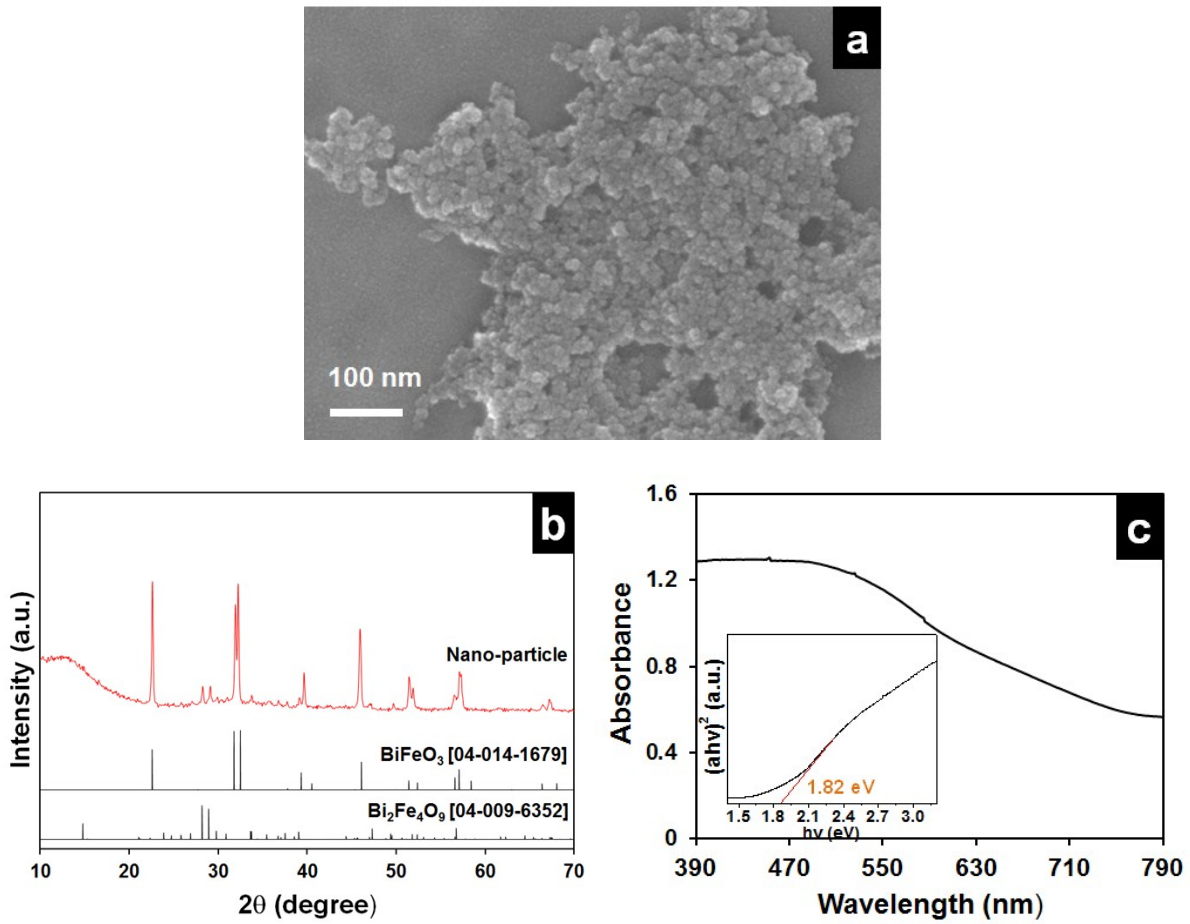

Fig. S2. SEM image of bismuth ferrite nanoparticles (a); XRD pattern of bismuth ferrite nanoparticles with perovskite and mullite crystalline phases (b); UV-vis absorption spectrum of bismuth ferrite nanoparticles and the corresponding Kubelka-Munk transformed reflectance spectrum (c).

For the hydrothermal treatment in co-solvent system, the effect of the different solvent ratios of methanol to water on the preparation of bismuth ferrites was investigated as well. As shown in Fig. S3, the prepared bismuth ferrites could be cube-like and pad-like shape with the reaction system of methanol and water, respectively. When the reaction system was replaced by co-solvent systems with the different ratios of methanol to water (i.e., 1:4, 1:1, or 4:1 v/v), the prepared samples will become cuboid-like shapes with a minor particle size change.

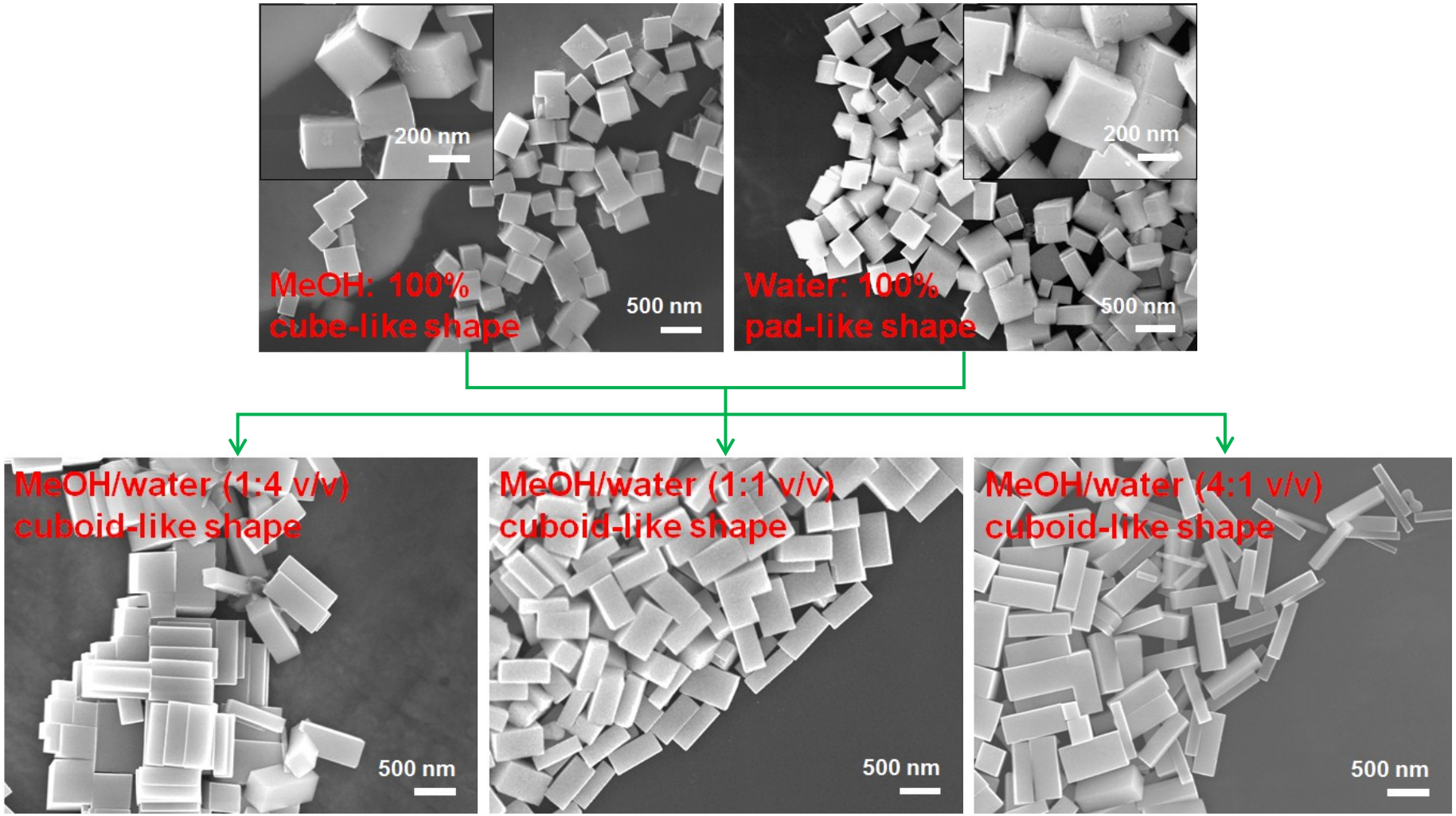

Fig. S3. SEM images of bismuth ferrites at different ratios of methanol/water by volume for hydrothermal treatment processes (conditions: holding 20 min at 200°C).

Fig. S4 shows the prepared bismuth ferrites with irregular morphologies when the reaction time is 5 or 120 min for the hydrothermal treatment processes. As shown in the figure (5 min), the bismuth ferrite nanoparticles are undergoing self-assembly, which possibly contribute to the gradual decomposition of citrate surfactants and the self-organization ability of bismuth ferrites under a high pressure and temperature. Moreover, with the increase of the reaction time for hydrothermal treatment, bismuth ferrites leads to formation of nanorods with nanocuboid in a slimline shape at the time of 120 min.

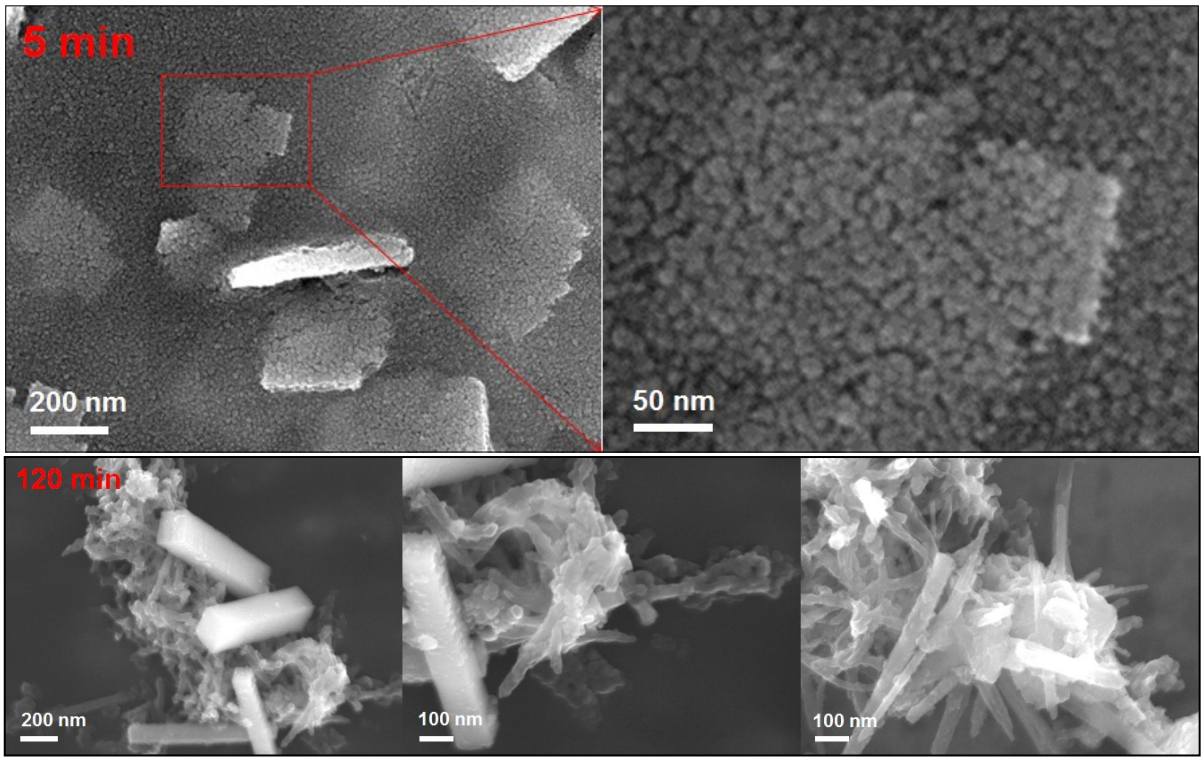

Fig. S4. SEM images of bismuth ferrites at different reaction time for 5 and 120 min during hydrothermal treatment processes.

As shown in Fig. S5a and b, the as-prepared bismuth ferrite nanoparticles could be used to prepare mullite bismuth ferrites undergoing conventional calcination processes. The corresponding reactions conditions are the ramping rate of 5°C min^{-1} and temperature of 700°C. As shown in Fig. S5a, the crystalline phase of bismuth ferrites could be mainly perovskite at the temperature below 500°C. It could be composed of mullite bismuth ferrites and sillenite bismuth ferrites at 600°C and further become mullite bismuth ferrites at a higher temperature of 700°C. The corresponding major characteristic peaks are marked in the figures. There is almost no significant influence of holding time from 12 to 24 h on the crystalline phase (Fig. S5b), but the prepared mullite bismuth ferrites have the poor morphology and particle size distribution with in the micron scale (SEM images shown in Fig. S5c). In addition, when the holding time was reduced to 20 min at temperature of 700°C, the prepared bismuth ferrites will be coexisting of mullite bismuth ferrites and perovskite bismuth ferrites (Fig. S5b). Hence, it seems that calcination is not an ideal method to prepare a relative pure bismuth ferrite because it needs higher temperature and longer holding times.

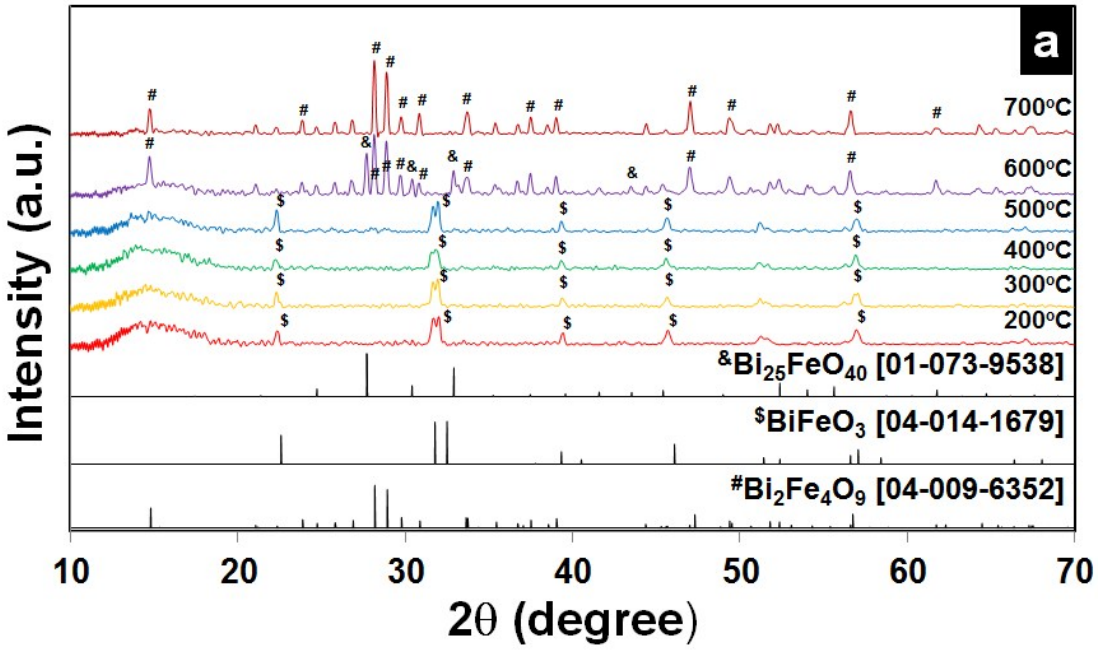

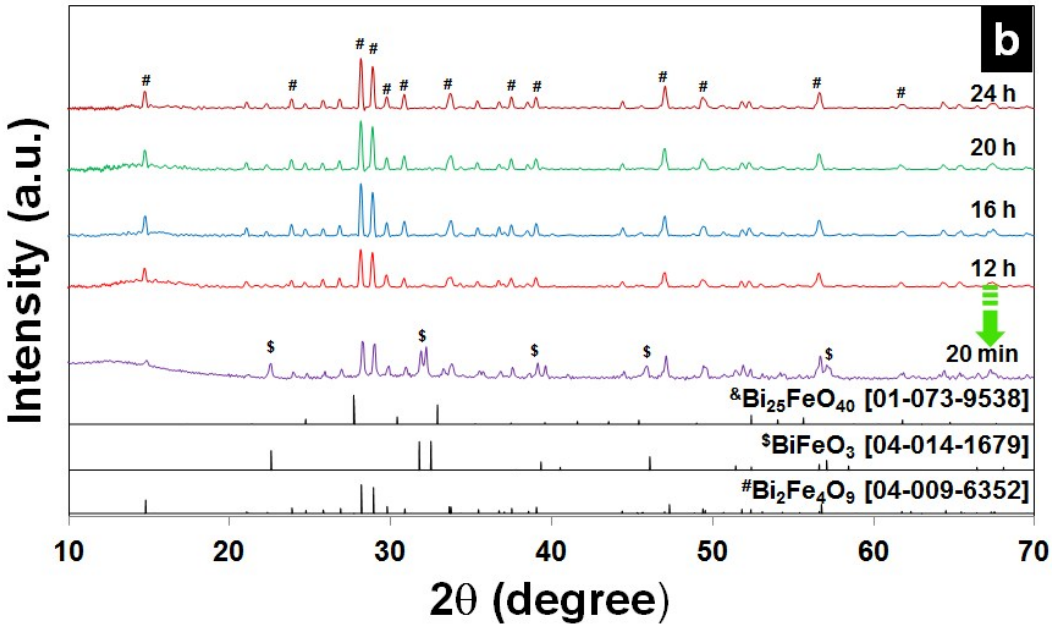

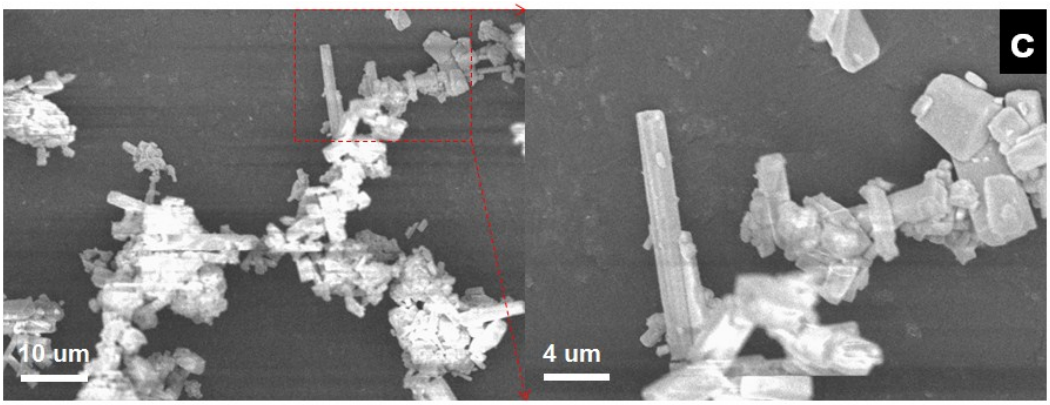

Fig. S5. XRD patterns marked with major characteristic peaks of the prepared bismuth ferrites under different temperatures with conditions of ramping rate of 5°C min^{-1} and holding time of 24 h (a); XRD patterns of the prepared bismuth ferrites under the different holding times with conditions of ramping rate of 5°C min^{-1} and temperature of 700°C (b); SEM image of the prepared mullite bismuth ferrites at temperature of 700°C for 24 h (c).

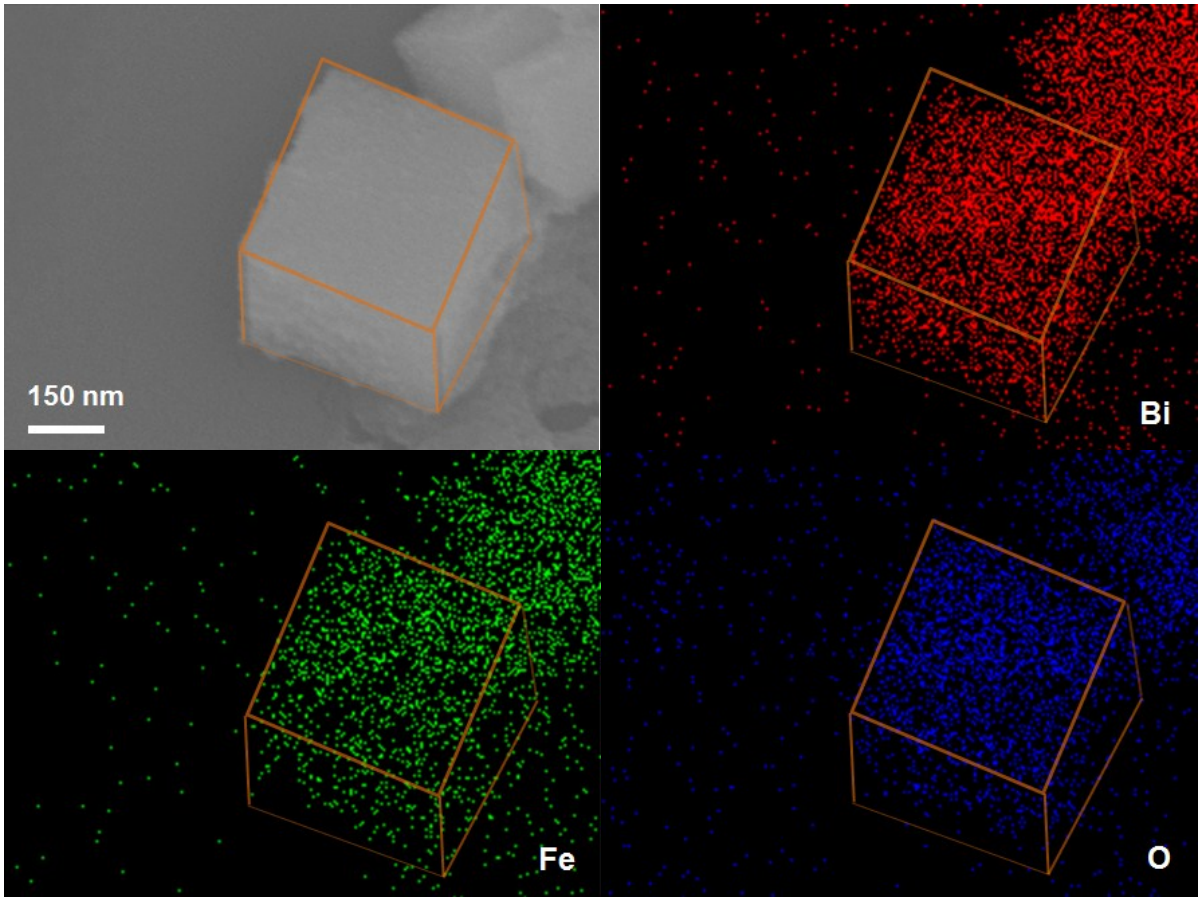

Fig. S6. SEM image of NSC-$Bi_2Fe_4O_9$ sample and the corresponding EDX elemental distribution mappings of Bi, Fe and O.

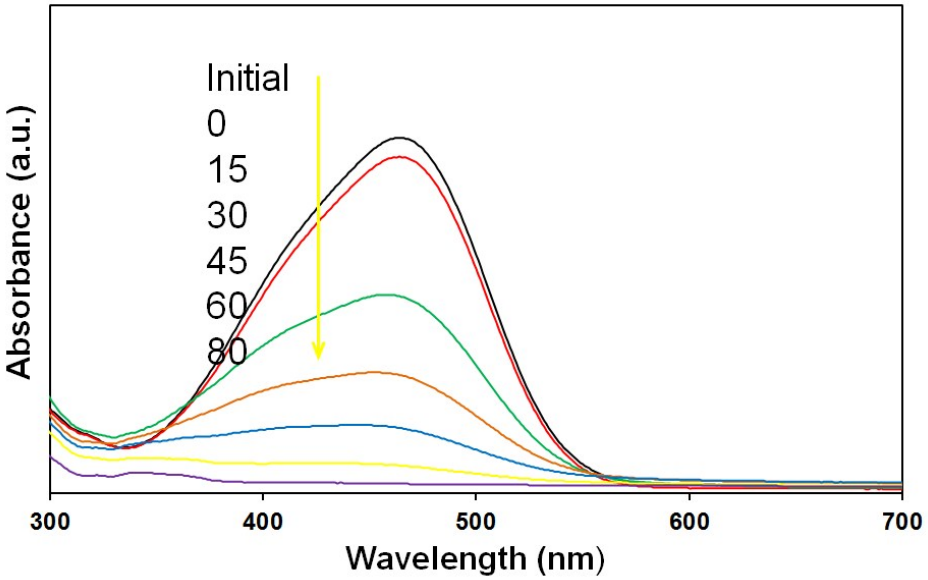

Fig. S7. UV-vis absorption spectra of MO degraded by NSP-$Bi_2Fe_4O_9$ within 80 min (The intensity at 0 min has slight change (~5%), which contributes to the adsorption of the pollutant on the catalyst surface at adsorption/desorption equilibrium status and suggests to neglect its adsorption capacity in this study).